Superconductivity as observed by Magnetic Resonance

Author: Anton Potočnik Mentor: izr. prof. dr. Denis Arčon

April 9, 2010

Abstract

Magnetic resonance techniques proved numerous times in the past to be a powerful tool in the investigation of the microscopic structure of the superconductors. NMR measurements of the superconducting state were the first to observe the divergences in the density of states on the edge of the energy gap, which is one of the main results of the BCS theory. Furthermore, NMR together with the ultrasound absorption measurements provided the first experimental prove for the existence of the Cooper pairs. After the discovery of the high-temperature superconductors NMR measurements still played a major role in the investigation of the microscopic superconductor structure, allowing for the determination of the wave-vector dependence of the energy gap, different pairing states and the effect of the strong electron-electron interaction, especially in the high-T_c superconductors.

1 Introduction

Superconductivity is today already widely used in many superconducting devices, namely high-field magnets, SQUID magnetometers, mass spectrometers and beam steering magnets in the particle accelerators [1]. Despite their wide use the theory of high-temperature superconductivity is still not entirely developed. Superconductivity was discovered in the 1911 by Kamerlingh Onnes, while studying the electrical resistivity of the mercury at the liquid helium temperatures. He observed that below critical temperature (T_c) the electrical resistivity of the material suddenly dropped to zero, within the experimental accuracy. Later it was found that the resistivity of the superconductors is absolute zero, meaning that the current in the insulated superconductor will flow indefinitely. Soon after the discovery of absolute zero resistivity, more non-intuitive phenomena were discovered in superconductors. Meissner and Ochsenfeld (1933) observed that applied magnetic field is expelled from the superconductor, which is now called the Meissner effect. Fritz London (1948) pointed out that the magnetic flux, surrounded by the superconducting material, is quantized and Josephson (1962) realized that in superconductors the interference effects span

to macroscopic distances [2]. Phenomena associated with the superconductivity caught the attention of many scientists, at that time and even today, since these effects manifest the quantum effects on a macroscopic scale.

Even-thought several superconducting properties had been known for long time it took almost 40 years after the discovery of the superconductivity that the first successful microscopic theory was developed by Bardeen, Cooper and Schrieffer, today known as the BCS theory. Their theory at that time explained all the non-intuitive superconducting phenomena and correctly predicted the results of many experimental investigations. The theory was thought to be a triumph of the superconductivity for many years up until the high-temperature superconductors were discovered in 1986 by Bednorz and Müller [3]. Although BCS theory failed to explain the experimental data measured on the high-temperature superconductors it provided a vital theoretical background for the future theories. The discovery of the high-temperature superconductors in addition opened up a new challenge of finding the room-temperature superconductors, which would have a mayor technological impact.

Throughout the course of the discovery of superconductivity magnetic resonance played a mayor role. Nulcear magnetic resonance (NMR), in particular, turned out to be a great local probe by providing the detailed microscopic magnetic picture of the superconductors. In order to understand the physics of magnetic resonance in superconducting state first the theory of magnetic resonance is needed for metal in the normal state. The first such theoretical approach was given even before the discovery of the NMR by Heitler and Teller [4] when they studied the possibility of cooling the sample using nuclear magnetic moments of the metal by adiabatic demagnetization. Later a complete theory of nuclear relaxation in metals was developed by Korringa [5], allowing thorough investigations of the superconductivity using magnetic resonance. And indeed, nuclear magnetic resonance turned out to be an indispensable tool for studying superconductivity, for instance it was the first to observe the divergences in the density of states (DOS) later explained by the BCS theory and by a combination with the ultrasound absorption it gave the first prove for the existence of the Cooper pairs [6]. With the high-temperature superconductors and lately discovered new families the NMR is still widely used [7], although the complete theory of high-temperature superconductivity is not yet known. Enriched by the BCS theory, the NMR measurements on high-temperature superconductors provide the determination of the DOS near Fermi level, electron pairing state, effect of the electron-electron correlations and more [6].

2 Normal metals

In magnetic resonance techniques studied sample is typically inserted into a strong applied magnetic field (max 9.4 T at IJS) where magnetic moments become polarized along the magnetic field direction. A strong pulsed electromagnetic signal (RF band, up to 400 MHz, in our NMR) is introduced perpendicular to the polarization direction, which rotates the magnetic moments away from

the main static magnetic field direction. The nuclear magnetic moments start to precess in the magnetic field, after RF pulses are switched of. The precession frequency in principle depends on the size of the magnetic moments and the external applied field ($\omega_0 = \gamma B_0$). Here gamma is the gyromagnetic ratio and is related to the nuclear magnetic moment through relation $\boldsymbol{\mu} = \gamma\hbar\boldsymbol{I}$. γ depends on the type of the nucleus. The variation of the measured precession frequency of a given nucleus in specific environment from ω_0 reflects the presence of internal magnetic fields, also called the shift on the resonance line. Due to the spin-lattice interaction the precessing magnetic moments loose energy and in a characteristic time T_1 return to the initial (thermal equilibrium) direction along the external magnetic field. The frequency shift from ω_0 and the T_1 relaxation time are typically measured quantities in NMR experiments which give information about the local structural and electronic properties.

In 1947, Knight [8] discovered in metals a characteristic resonance frequency shift ($\mathcal{K} = \frac{\omega-\omega_0}{\omega_0}$), called the Knight shift. The shift comes from the hyperfine interaction between the nuclei and conducting electrons. The electron in the s-orbitals, where the probability of electrons being on the nucleus site is non-zero, interacts with the nucleus with the Fermi contact interaction $V \propto \langle \boldsymbol{\mu}_n \cdot \boldsymbol{\mu}_e \rangle \, \Psi^2(0)$. Were $\boldsymbol{\mu}_n$ and $\boldsymbol{\mu}_e$ are the nuclear and electron magnetic moments. The electron magnetic moment can be in an approximation replaced by the average electron magnetic moment, which is in metals proportional to the conducting electron spin susceptibility χ_s (or Pauli susceptibility),

$$\mathcal{H} = \boldsymbol{\mu}_n \cdot \boldsymbol{H} + A\,\boldsymbol{\mu}_n \cdot \langle \boldsymbol{\mu}_e \rangle = \boldsymbol{\mu}_n \cdot \boldsymbol{H} + A\,\boldsymbol{\mu}_n \cdot \chi_s \boldsymbol{H} = (1+\mathcal{K})\boldsymbol{\mu}_n \cdot \boldsymbol{H}.$$

Thus, $\mathcal{K} = A \cdot \chi_s$ directly measures local spin susceptibility. Pauli susceptibility is further proportional to the density of states at Fermi energy [9]. The Knight shift therefore depends on the density of states at Fermi energy,

$$\mathcal{K} \propto \chi_s \propto \rho\,(E_F)\,.$$

In metals DOS does not change considerably with temperature. A constant Knight shift over a large temperature interval therefore provides an indication for a metallic state.

Three years later Korringa [5] calculated the NMR relaxation rate for a simple metals, which related the Knight shift with the T_1. The formula is now called the Korringa relation,

$$T_1 T \mathcal{K}^2 = \frac{\gamma_e^2}{\gamma_n^2} \frac{\hbar}{4\pi k_\mathrm{B}} K_P \tag{1}$$

were γ_e and γ_n are electron end nuclear gyromagnetic ration, $\mathcal{K}$ is the Knight shift and k_B is the Boltzmann constant. This relation was verified and studied extensively by the experiments particularly on the alkali metals [10]. It was soon found [11] that Korringa relation does not hold exactly when electron-electron interactions are important. The formula can be corrected by adding a constant factor, K_P to the right hand side of the relation, which is less than

one for anti-ferromagnetic electron-electron correlations and is more than one for the ferromagnetic correlations. It is interesting to note that in the case of no electron-electron interactions the left hand side of the Korringa relation (Eq. 1) depends only on the fundamental constants, i.e. $K_P = 1$, and it does not depend on the material in which the nuclei reside.

If the Knight shift is temperature independent, which is typical for metals, the Korringa relation can be rewritten as

$$\frac{1}{T_1} \propto T$$

which is also known as the Heitler-Teller equation. This equation can be easily derived by realizing that the *nuclear relaxation in metal may be viewed as a scattering process*, where electrons are scattered by the nuclear magnetic moments, flipping the nuclear spin in the process. Considering electron-nuclear interaction to be hyperfine, scattering can be imagined as when the electron comes close to the nucleus both their spins precess around the resultant total spin angular momentum vector, leaving the scattering process both with changed spin orientation. If we treat the electrons as free electron gas and the hyperfine interaction as Fermi contact interaction ($V(\mathbf{r}) = 8\pi/3\gamma_e\gamma_n\hbar^2\delta(\mathbf{r})$), where scattering is independent of the direction of the electron velocity, a simple quantum mechanical theory of the T_1 can be derived. Let us assume that after the scattering the nuclear spin and electron spin are changed as well as electron wave vector is changed from k to k'. The scattering can be derived using the Fermi's Golden Rule: the probability per second of a transition of an electron from the initial state i to the final state f is

$$W_{if} = \frac{2\pi}{\hbar} \left| \left\langle i \left| \hat{V} \right| f \right\rangle \right|^2 \delta(E_f - E_i - \Delta E)$$

where $\hat{V}$ is the hyperfine coupling energy operator and ΔE is the change in the nuclear spin Zeeman energy. In order the transition can take place the initial state must be occupied and the final state must be empty. We sum over all initial states weighted by the probability for the occupied states ($F(E_i)$) and over all final states weighted by the probability for the unoccupied states ($1 - F(E_f)$). The sums can be replaced by the integrals, denoting the number of states within $\mathrm{d}E$ at energy E as $\rho(E)\mathrm{d}E$. Assuming the ΔE is much smaller than the thermal energy, $k_\mathrm{B}T$, the energy difference can be neglected and the probability for the transition can be written as

$$W = \frac{2\pi}{\hbar} \int \left| \left\langle i \left| \hat{V} \right| f \right\rangle \right|^2 F(E_i) \left(1 - F(E_i)\right) \rho\left(E_i\right)^2 \mathrm{d}E_i. \tag{2}$$

At low temperatures the term $F(E_i)\left(1 - F(E_i)\right)$ can be approximated by the delta function. In the limit where changes of $\left| \left\langle i \left| \hat{V} \right| f \right\rangle \right|$ and $\rho\left(E_i\right)$ can be neglected over the energies comparable to $k_\mathrm{B}T$ we can come to the final from,

$$\frac{1}{T_1} = W = \frac{2\pi}{\hbar} \left| \left\langle i \left| \hat{V} \right| f \right\rangle \right|^2_{E_\mathrm{F}} \rho\left(E_F\right)^2 k_\mathrm{B}T \tag{3}$$

where subscript E_F means evaluation at Fermi energy. The linear dependence comes from the fact that electrons within about $k_\mathrm{B}T$ of the Fermi surface are scattered by the nuclear magnetic moment, which is only a fraction of the total number of electrons of the order of (k_BT/E_F).

3 Superconductivity

3.1 Type I and type II superconductors

There are two types of superconductors characterized by the two distinct lengths. The magnetic field penetration length λ, a typical length that magnetic field penetrates the SC state, and correlation length ξ, sometimes called also Cooper-pair length. The former can be easily obtained using the second London equation [12] ($\nabla \times \mathbf{j}_s = -\frac{n_s e^2}{mc}\mathbf{B}$) and the Ampere's law ($\nabla \times \mathbf{B} = 4\pi\mathbf{j}/c$) yielding,

$$\nabla^2\mathbf{B} = \frac{1}{\lambda^2}\mathbf{B} \qquad \lambda = \sqrt{\frac{mc^2}{4\pi n_s e^2}},$$

where m is electron mass, n_s density of superconducting electrons and e electron charge. λ is a characteristic length of a layer of normal state surrounding the superconducting state for a superconductor in an external magnetic field, where magnetic field is not entirely expelled by the Meissner effect. The energy gain of having magnetic field in this region is $\propto \lambda^2 H^2$ per unit volume.

The concept of the correlation length was first introduced by Ginzburg and Landau [13] where correlation length is described as a stiffness of the superconducting wave function. Later Pippard [14] who was doing experiments on microwave electrical conductivity gave the name correlation length and estimated its value from the uncertainty principle to,

$$\xi = \frac{a\hbar v_F}{k_B T_c}.$$

Here a is a constant of the order of unity, v_F the velocity of electrons at the Fermi energy and T_c the superconducting transition temperature. The energy gain of having a superconducting state is consequently $\propto \xi^2 H_c^2$ per unit volume, which can be seen also as a bounding energy of Cooper pairs.

In conventional superconductors penetration depth (typical 100 nm) is much shorter than the correlation rate ($\lambda/\xi \ll 1$). Comparing the energy scales of the normal and superconducting state, one sees that when $B < B_c$ normal state is expelled by superconducting state and when $B > B_c$ the superconducting state is destroyed. Such materials were later named *type I superconductors*. Abrikosov (1957) [15] showed, that for a case when $\lambda > \xi$ the situation is drastically different. When $B < B_c$ like in type I superconductors normal state is expelled by the superconducting state, however when $B > B_{c1} = (\xi/\lambda)\, B_c$ the superconducting state is considering above energy estimations energetically not favorable. By noticing the energy contribution of the interface between the

two states, a normal state filaments, also called vortexes, are formed in this range (see Fig. 1). With the increase of the magnetic field the density of the vortexes is increased up until the vortex separation is of the order of correlation length. Higher magnetic fields cross the border of B_c where superconductivity is destroyed and only normal state remains. Such superconducting materials are called *type II superconductors*.

NMR measurements on the type I superconductors are possible on thin films or fine particle samples where at least one dimension is smaller than λ. Another possibility is to use pulsed high magnetic fields ($B > B_c$), during which the magnetic moments in the normal state get polarized and measured in the subsequent pulse, but the relaxation happens in the superconducting state between the pulses, where $B < B_c$. Type II superconductors present no such challenge since in the mid range $B_{c1} < B < B_c$ material consists of both the superconducting and the normal state regions. The nuclear moments get polarized in the normal state filaments and are relaxed by superconducting electrons in close proximity in superconducting state or by the on-site superconducting electrons when the filament is moved away. The nuclear moments are relaxed also by the normal state electrons, however this can be subtracted since the relaxation in metals is known from the Korringa relation. The typical values for critical fields for the type II superconductors are $H_{c1} = 40\,\mathrm{mT}$ and $H_c = 30\,\mathrm{T}$ (in Nb_3Sn) [2].

3.1.1 Fluxuid lattice

The magnetic flux lines in type II superconductors form a lattice. It was long debated weather the flux lattice is square or triangular, until it was experimentally determined using NMR [16] that the flux lattice is triangular. The NMR lineshape is strongly dependent on the surrounding magnetic field distribution, which is observed through the NMR spectrum. A comparison between the calculated triangular and square vortex lattice NMR spectra is depicted in Fig. 1a. The NMR spectrum directly measures the local magnetic field distribution felt by nuclei, which are in this case equally distributed over the vortex structure. The so-called Redfield distribution comes from different magnetic fields between vortex centers, where magnetic field is maximal (points V in Fig. 1a) and points in-between vortexes (points C), where magnetic field is minimal. There is also a third characteristic point - a saddle point in magnetic field (points S), where distributions diverges. The position of this point differs for triangular and square lattices in the magnetic field distribution, thus allowing the determination of the vortex lattice symmetry. However, direct picture of the flux lines cannot be obtained by the NMR method. For this purpose scanning microscopic techniques are more frequently used (Fig. 1b).

Since flux lines are filament-like areas of non-superconducting state a standard Korringa relation should hold for the nuclear relaxation. Contribution to the relaxation rate in type II superconductors should therefore be of the order of $(1/T_1)_{\mathrm{Korringa}} \cdot n\pi\xi^2$, where n is the density of the flux lines per unit area, $n = B/\phi_0$ and discrete flux unit $\phi_0 = h\,c/2e$ passing through a flux filament. These contribution was indeed experimentally observed [19] and yielded a rea-

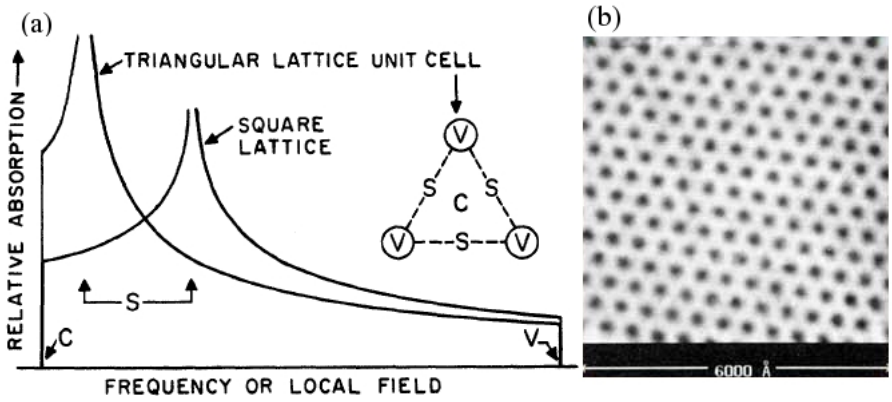

Figure 1: (a) Calculated NMR spectrum of triangular and square vortex lattice. Point V corresponds to the large magnetic field inside vortexes, point C corresponds to magnetic field between the vortexes and point S corresponds to the magnetic field saddle points [18]. (b) STM image of a triangular vortex lattice [17].

sonable value for ξ. A precise value of ξ cannot be obtained since there is no quantitative theory so far, which would hold for such systems.

3.2 Bardeen-Cooper-Schrieffer Theory

3.2.1 Energy Gap

Energy gap Δ is perhaps one of the most important parameters characterizing superconducting state. In order to break Cooper pairs and create excitation energy of at least 2Δ is required. The energy gap in superconductivity was first introduced by John Bardeen (1954) who at that time developed a simple model that he believed will give the Meissner effect and thus explain superconductivity. In his model a gap in the density of states appears right at the Fermi energy as soon as material becomes superconducting (Fig. 2b). He argued that the energy gap should be approximately $k_B T_c$.

The idea of energy gap at the Fermi energy motivated C.P. Slichter to measure T_1 in the superconducting state [6] since according to Korringa relation (Eq. 3) T_1 in metals strongly depends on the density of states at the Fermi level. Slichter together with Hebel succeeded to measure T_1 in the superconducting state of aluminium almost five years later [20]. Since at that time only type I superconductors were known, they used the pulsed high magnetic field technique on Al (Fig. 3), which was known to have a long relaxation time compared to other metals. In these experiments the relaxation time needed to be significantly longer than the high magnetic field pulse repetition time, otherwise all magnetic moments would be realigned to the initial position already in the normal state before the measuring pulse would occur. Another serious problem

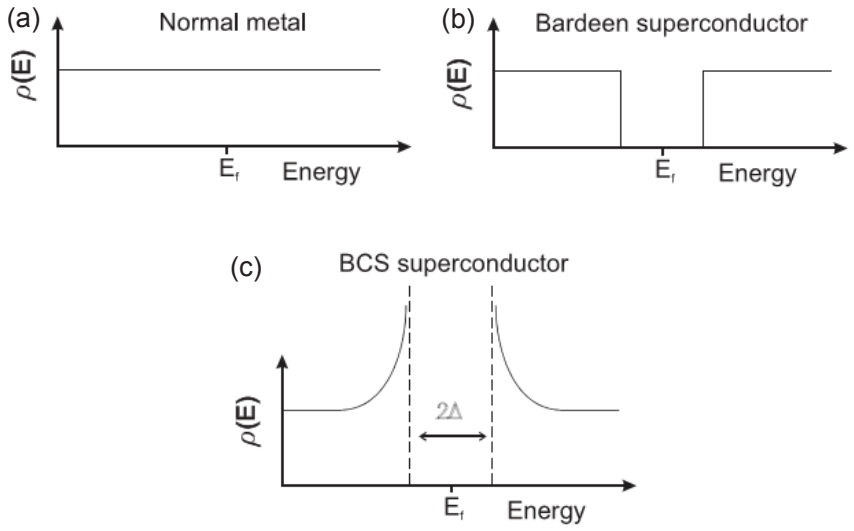

Figure 2: Density if states for normal metal (a), for Bardeen model (b) and the BCS model (c).

that they faced was the low T_c of aluminum (1.172 K). Using liquid He one can cool down to 4.2 K (He boiling point) and by decreasing the pressure a temperature of 1.2 K can be reached. Cooling below this point is prevented by an effect called Rollin film typical for superfluid ^{4}He, however using triple Dewar system they succeeded in reaching 0.9 K [6].

The results of their T_1 measurements are depicted on Fig. 4. Following the simple model density of states proposed by Bardeen (Fig. 2b) for the superconducting state one would expect $1/T_1$ to drop below T_c according to $\exp(-2\Delta/k_BT)$. However, much to their surprise Hebel and Slichter noticed that $1/T_1$ in the superconducting state at first unexpectedly increases and later decreases following $\exp(-2\Delta/k_BT)$. The peak in the $1/T_1$ temperature dependence below T_c is now called *the Hebel-Slichter peak*. When examining their data Hebel and Slichter thought of one possible explanation. Since $1/T_1$ depends on the density of states the peak could be a consequence of the increase of density near the gap edges. The BCS theory later showed an analogous shape of the density of states as suggested by Hebel and Slichter (Fig. 2c).

Some of the superconducting materials do not exhibit energy gap [21]. These are typically materials with magnetic impurities, which effectively reduce the life time of quasi-particles. Finite quasi-particle lifetime leads to the smearing of the energy. It is surprising that even without energy gap these materials have zero resistivity in the superconducting state. Strictly speaking, all superconducting materials are gap-less, since BCS theory is only an idealization and in reality all excitations have finite lifetimes and therefore finite density of states at zero energy. Density of state is many orders of magnitude smaller than in normal

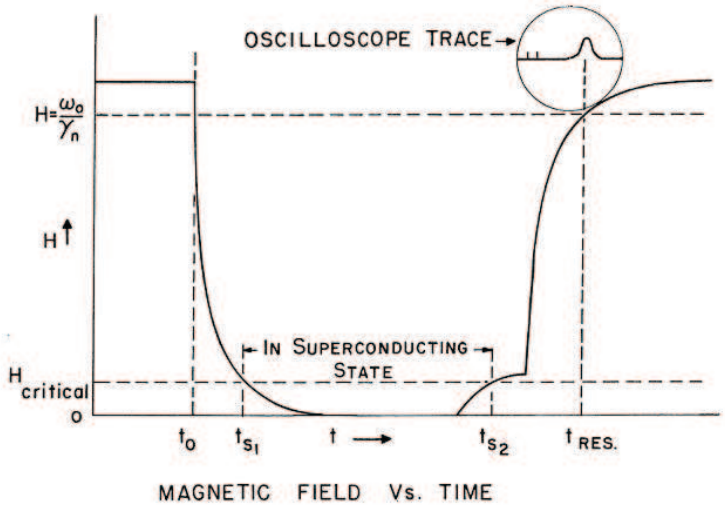

Figure 3: Hebel-Slichter field cycling experiment [6].

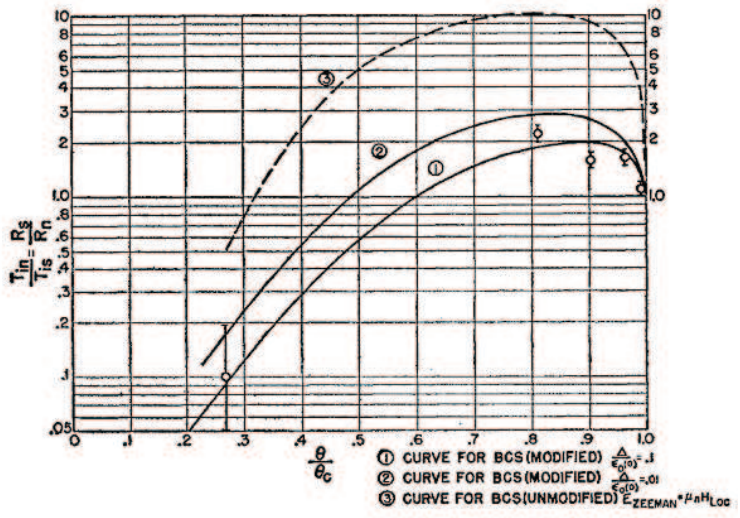

Figure 4: Relaxation rate in superconducting state, normalized by the value at T_c [20].

state, where in the gap-less SC it is of the same order. An example of gap-less superconductors are type II superconductors near T_c. It was observed experimentally that at higher magnetic fields T_1 no longer gets smaller just below T_c but instead gets longer.

There are several methods of measuring the energy gap in superconductors besides NMR, however NMR measurements prove to be simple, easy and reliable. For example, when energy gap is measured by specific heat measurements small impurity phases, typically non-SC, cause large errors, but they hardly contribute to the T_1 relaxation at longer times. Energy gap can be measured also using electron tunneling microscope. Unfortunately the measurements are accurate only in pure materials, where coherent length is long. Measurements on materials with much impurities, yield information about the surface rather than about the bulk [22]. The drawback of the NMR T_1 method is it's dependence on the magnetic field, which can destroy the SC state if to high. For this reason measurements on type I superconductors are often conducted in a pulsed magnetic field and measurements on type II superconductors in lower magnetic fields.

3.2.2 Cooper pairs

After the discovery of the isotope effect on the superconducting transition temperature (T_c) Bardeen and Pines started to investigate the electron-phonon interaction and the interaction of the two electrons mediated by the lattice distortion [23]. However, it was Cooper, the Bardeen's post doctoral associate, who made an important discovery. He considered two electrons with energies above filled Fermi level to have an attraction interaction and found that such electrons would form a bound state ($\boldsymbol{k}$, spin $\uparrow$; -$\boldsymbol{k}$, spin $\downarrow$). These so-called Cooper pairs were the key to understanding the lifting of degeneracy in metals and consequently the formation of the energy gap. The complete theory of superconductivity required to include all electrons, not just one pair above the Fermi surface. The problem was solved by Schrieffer who found out that the wave function of superconducting state is made up entirely of Cooper pairs in which each pair state was occupied fractionally [6]. Employing the Schrieffer's wave function, Bardeen, Cooper and Schrieffer solved the Hamiltonian, first at zero temperature and then soon extended the analysis to temperatures up to transition temperature. They found that the energy gap varies with temperature and vanishes at T_c, when the transition to normal state occurs. They derived the relation between energy gap and T_c for weak coupling between the electrons to be

$$2\Delta(0\,\mathrm{K}) \approx 3.52\, k_B T_c, \tag{4}$$

where 2Δ is the difference between the upper and the lower gap edges. They were able to calculate the results of many experiments with great accuracy including the Hebel-Slichter peak and the $1/T_1$ dependence at lower temperatures,

$$1/T_1 \propto \exp\left(-\Delta(T)/k_B T\right). \tag{5}$$

One of the greatest mysteries concerning the conventional superconductivity was that the measurements of ultrasound absorption in the superconducting state do not exhibit the Hebel-Slichter peak just below T_c even-though the scattering mechanism is the same as in the NMR T_1 relaxation and the same arguments that we used to derive Eq. 3 should hold. The only difference is that in ultrasound absorption the superconducting electrons are scattered on the phonons, which change only the superconducting electron's wave vectors, whereas in NMR SC electrons are scattered on the nuclear moments, where also a flipping of the superconducting electron's spin occurs. One of the great triumphs of the BCS theory was to explain this difference. The explanation is considered to be one of the best proofs for the pairing mechanism. To give a short explanation let us consider Eq. 2. The difference between the sound absorption and nuclear relaxation is the spin flipping in the later case and since Cooper pairs consist of two electrons, one with $\boldsymbol{k}$ and spin up and other with $-\boldsymbol{k}$ and spin down, there are two matrix elements that join any initial state to the same final state. Denoting these as $\hat{V}_1$ and $\hat{V}_2$ we should replace $\hat{V}$ in Eq. 2 with ($\hat{V}_1$+$\hat{V}_2$) for NMR and ($\hat{V}_1$-$\hat{V}_2$) for ultrasound. The density of states according to the BCS theory is [6]

$$\rho_s(E) = \frac{\rho_n(E)\sqrt{E}}{E^2 - \Delta^2},$$

where ρ_n is the density of states in normal metals. We see that when $E = \pm\Delta$ density of states diverges as predicted by Hebel and Slichter. The square of the matrix element for the ultrasound between states at E and E' goes as $EE' - \Delta^2$, whereas for the NMR the square of the matrix element goes as $EE' + \Delta^2$. This correction is called coherence factor. We can now see that in the case of the ultrasound absorption singularity in density of states cancels out by the matrix elements and thus no peak is observed. On the other hand, the singularity remains in the nuclear relaxation which results in the Hebel-Slichter peak.

In the BCS theory the superconductivity is explained by the effect that the lattice phonons have on the electron-electron interaction. The energy gap parameter $\Delta_{\boldsymbol{k}}$ in the BCS theory is the solution of an integral equation and is in general a function of wave-vector. However, BCS approximated the energy gap parameter to a scalar value Δ_0 for electrons in some cutoff region around Fermi level and set to zero outside this region. In BCS energy gap is independent on the wave-vector. The theory is, on the other hand, more general. Depending on the electron-electron interaction, other pairings are possible. In a situation of zero electrical current flow, the electron momentum is zero, however electron pairs can have a non-zero angular momentum about their mass centers with quantum numbers $L = 0$, 1, 2, etc. Due to the Pauli exclusion principle the total wave function has to be antisymmetric for the electron exchange, allowing only two spin quantum numbers: $S = 0$ for even L and $S = 1$ for odd L. The possible BCS states therefore are the standard BCS state ($L = 0,\ S = 0$) called the s-wave superconducting state and higher unconventional states: p-wave superconducting state ($L = 1,\ S = 1$), d-wave pairing state ($L = 2,\ S = 0$), etc. For example, d-wave pairing state is believed to be the case in cuprates,

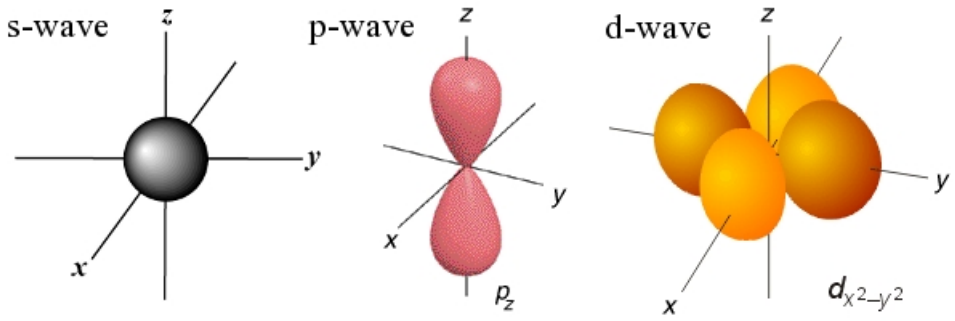

Figure 5: s-wave, p-wave and d-wave symmetries.

the high-T_c superconductors. After solving the Hamiltonian with given pairing states the energy gap turns out to be isotropic in $\boldsymbol{k}$-space in the s-wave superconductors and anisotropic in p- and d-wave superconductors with a specific $\boldsymbol{k}$ dependence (see Fig. 5). The pairing symmetry can be in fact directly measured using certain tunneling experiments [24] or by a typical power-law dependence of $1/T_1$ below T_c.

4 Alkali Doped Fullerides

Soon after the discovery of C_{60} molecule it was found that triply doped fullerides with the alkali metals (A_3C_{60}) exhibit type II superconductivity [25] with remarkably high T_c's, for example 19.5 K for K_3C_{60}, 29.5 K for Rb_3C_{60} and 31 K for Rb_2CsC_{60}. To some extend this is expected since large molecules have many phonon modes which are required for the conventional BCS superconductivity. For this reason structural, electronic and superconducting properties of fulleride superconductors have been extensively studied over the last couple of decades [26]. Fulleride superconductors also show another striking feature, namely the superconducting transition temperature is scaled with the inter-fulleride separation (Fig. 6a). This is easily explained within the framework of BCS theory, where for non-interacted electrons critical temperature is given by [26]

$$k_B T_c = 1.13\hbar\omega_{\mathrm{ph}} \exp\left(-\frac{1}{N(E_F)V}\right). \tag{6}$$

Where ω_{ph} is Debuy frequency, V electron-phonon interaction matrix element and $N(E_F)$ density of states at Fermi energy. By increasing of the inter-fulleride distance, either by doping with larger anions or by the reduction of applied pressure, results in the smaller overlap of the electron orbitals between the neighboring C_{60}^{-3} anions. Reduced overlap results in a smaller band width and consequently yields higher density of states, which according to the Eq. 6 increases T_c.

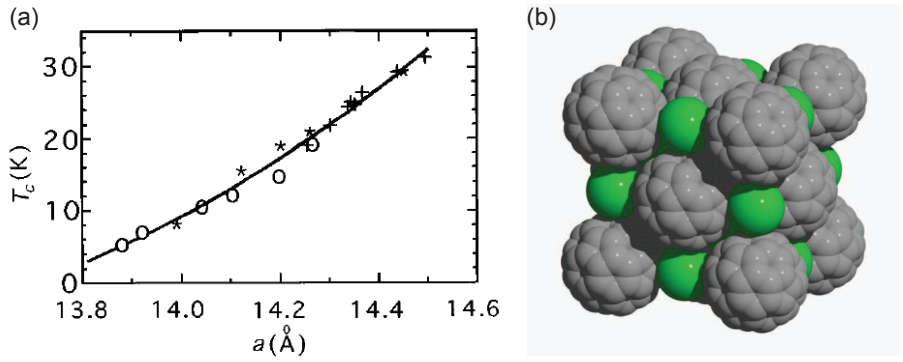

Figure 6: (a) T_c dependence on the lattice size [26]. (b) A_3C_{60} crystal structure.

Following this feature T_c seems to increase indefinitely with increasing lattice parameters. However, at some large unit cell volume, where on-site Coulomb repulsion becomes relevant this prediction is expected to break-down. It has been experimentally realized only very recently in hyper-expanded fulleride Cs_3C_{60} where a non-superconducting and an antiferromagnetic insulating state at ambient conditions have been observed [7]. It's phase diagram is remarkably similar to that of other high-T_c superconductors and signals that in expanded lattices electron-electron correlations play an important role. In this section we will focus only on the non-hyperexpanded alkali doped fullerides, such as K_3C_{60} and Rb_3C_{60}.

The NMR T_1 measurements on a typical alkali doped fulleride (Rb_3C_{60}) are shown in Fig. 7a. In the normal state (above 30 K) $1/(T_1T)$ slightly increases with increasing temperature and is temperature independent above $\sim 150\,\mathrm{K}$. This is reminiscent to simple metals where due to the Korringa relation $1/(T_1T)$ should be constant. Similar results were observed also in other A_3C_{60} superconductors [27, 28], but not in Cs_3C_{60} [29]. In the superconducting state $1/T_1$ drops exponentially with decreasing temperature as expected for the creation of the energy gap. The fit to the low temperature T_1 measurement (Fig. 7b) is in a reasonable agreement with the BCS-derived formula for $1/T_1$ (Eq. 5). The fit to the measurements on K_3C_{60} and Rb_3C_{60} yield the quotient $2\Delta/k_BT_c^{\mathrm{NMR}}$ of 3.0 and 4.1, respectively. This is in a rough agreement with the calculated BCS value (3.5; see Eq. 4), showing that the discussed alkali doped fullerides are conventional s-wave superconductors. One can see that the measurements show no Hebe-Slichter peak near T_c. It was known from the studies of V_3Sb [30] that a static magnetic field (typical for type II SC) may suppress the coherence peak. Experiments in lower magnetic fields (including zero-field muon spin relaxation measurements) indeed observed the recovery of Hebel-Slichter peak below certain applied field [28].

The Knight shift is also a valuable quantity that provide much information regarding the magnetism of the sample. The electrons in $S = 0$ singlet state

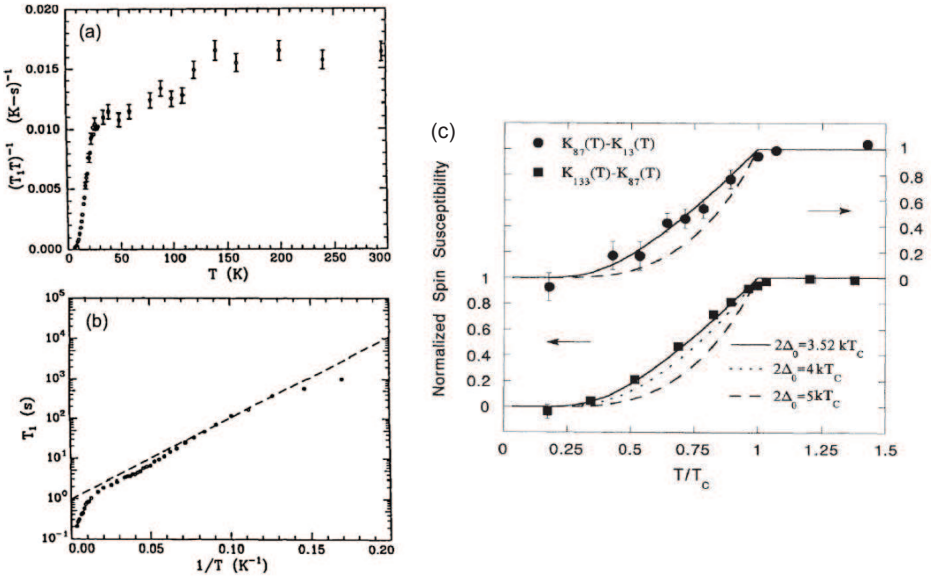

Figure 7: (a) NMR $1/T_1T$ measurements on Rb_3C_{60}. (b) Inverse Temperature dependence of T_1 in log scale shows a good agreement with BCS s-wave superconductivity. (c) Electron spin susceptibility from the Knight shift and theoretical lines for different $2\Delta/k_BT_c$ quotients. [6]

cannot interact with an applied magnetic field nor with the nuclear moment, measured in NMR. Consequently the Knight shift should vanish in the superconducting state at $T = 0$. This holds only for s- and d-wave superconductors with a zero spin quantum number, S. However, in type II superconductors, Meissner diamagnetism may overshadow the vanishing χ_s thus making the analysis ambiguous. In fact, measured Knight shift seldomly vanished due to, for example, the remaining magnetic field present in the type II superconductors. The problem can be bypassed by subtracting the Knight shifts of two species in the compound, (e. g. ^{13}C and ^{87}K in K_3C_{60}), influenced by the same remaining magnetic field, i.e. diamagnetism is the same for both nuclei. Normalized spin susceptibilities obtained by a subtraction of the Knight shifts for different nuclei are depicted in Fig. 7c. In this method Stenger found the best agreements between calculated values and measured data when the weak-coupling BCS value is $2\Delta/k_BT_c^{\mathrm{NMR}} = 3.52$, which was another evidence that A_3C_{60} are conventional s-wave superconductors.

5 Cuprate Superconductors

As a contrast to the conventional superconductors the high-T_c cuprate superconductors (type II) will be presented in this section. Discovered in 1986 by

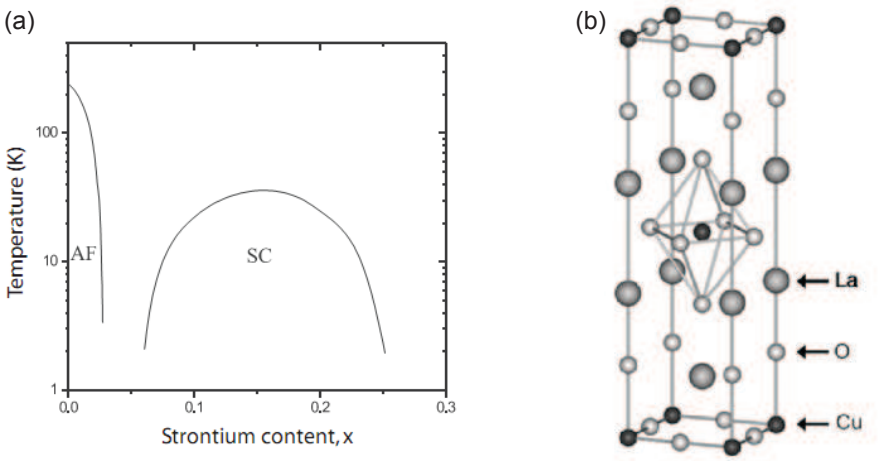

Figure 8: (a) Phase diagram and (b) crystal structure of $La_{2-x}Sr_xCuO_4$[6]

Bednorz and Müller [3] their superconductivity is still not entirely understood. There are several features that distinguish them from the conventional SC, the high transition temperature (current record: $T_c = 135$ K in $HgBa_2Ca_2Cu_3O_x$) [1], antiferromagnetic insulator ground state of parent compounds and a layered - largely anisotropic structure (Fig. 8a-b). In cuprates superconductivity arises for example after the doping with strontium atoms in $La_{2-x}Sr_xCuO_4$, where x denotes the amount of dopand. The facts that the parent compound (undoped compound) is an antiferromagnet at low temperatures and an insulator despite the half-empty conduction band, highlights the immense importance of the electron-electron interaction in cuprates.

From the early NMR measurements it became soon apparent that the normal state of the cuprate superconductors is no ordinary metal. For example, the Knight shift is temperature independent in metals, wheres it is almost a linear function of temperature in cuprates (Fig. 9a). Moreover, the $1/T_1$ is a linear function of temperature in metals, compared to the cuprates where it saturates at a certain temperature and remains constant above this temperature (Fig. 9b). Another unexpected feature is linear dependence of T_1T and the up turn at low temperatures as seen in Fig. 9c, which is a signature of phenomenon called *the pseudo gap*. Here nuclear moments are relaxed by coupled electrons that form a singlet-triplet state. In the singlet ground state electrons do not couple to the nucleus, whereas in the triplet state they do. At temperatures lower than singlet-triplet splitting (still above T_c) electron pairs will preferentially be in the ground singlet state and thus nuclear moments will not be relaxed, leading to an upturn in T_1T data.

In the superconducting state the Knight shift decreases with temperature (Fig. 9a) indicating the singlet ground state. The $1/T_1$ does not drop to zero exponentially, as expected for conventional superconductors, but rather seems

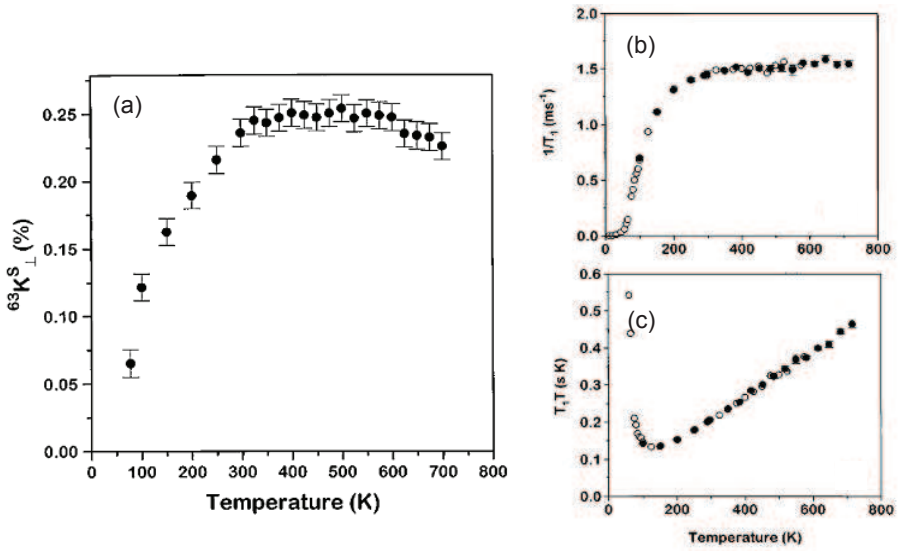

Figure 9: (a) ^{63}Cu Knight shift in the direction perpendicular to the crystal c axis. (b) ^{63}Cu spin lattice relaxation rate. (c) T_1T as a function of temperature. [31]

to fit the power law at low temperatures (Fig. 10a)

$$1/T_1 \propto T^3.$$

In Fig. 10b $T_1(T_c)/T_1(T)$ is plotted against T_c/T in log-scale, which reflects the temperature dependence of the energy gap. It can be seen that data of cuprates do not follow the BCS s-wave line. The slope of the data continuously change with temperature, getting smaller with temperature. At high temperatures there are excitations in a broad $\boldsymbol{k}$-space interval, whereas at low temperatures the excitations are only in a small interval where the energy gap is smaller. This would indicate that in cuprates the energy gap is strongly anisotropic and depends on the wave-vector, in a contrast to the conventional BCS superconductors. The pairing state in cuprates is therefore not an s-wave, but must be higher, p- or d-wave state. However, the Knight shift measurements show a spin singlet ground state, ruling out the p-pairing state ($L = 1,\ S = 1$). The most likely symmetry of the Cooper pairs in the cuprate superconductors is therefore the d-wave symmetry, which is now generally accepted. The NMR gave one of the earliest evidence for the existence of d-state pairing [6].

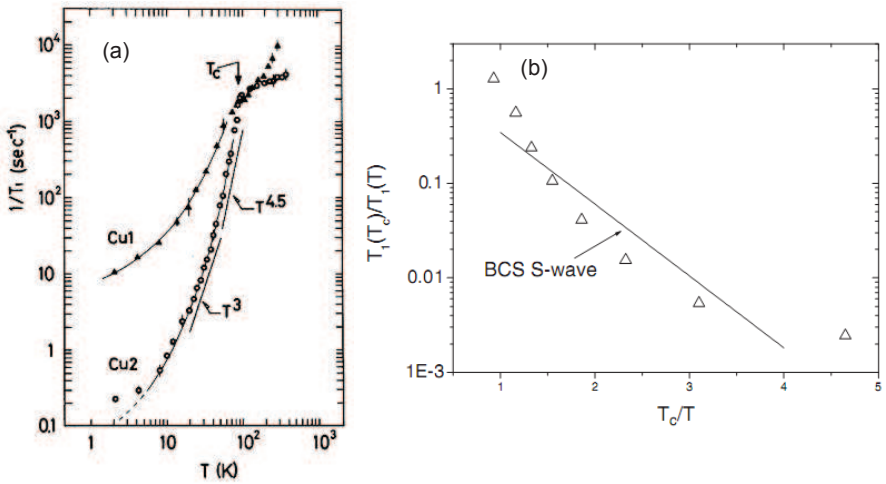

Figure 10: (a) Temperature dependence of the ^{63}Cu relaxation rate in the log-log scale [32]. (b) Normalized relaxation rate as a function of normalized reciprocal temperature [33].

6 Conclusions

The complete understanding of the superconductivity is vital since the effect has a large technological potential. The nuclear magnetic resonance was one of the first techniques used for the investigation of superconductivity since it provides a unique insight into a local magnetic structure in the vicinity of the observed nucleus. It played an essential role in the experimental confirmation of the existence of the energy gap and the Cooper pairs - central objects of the BCS theory. With the discovery of the high temperature superconductors the magnetic resonance techniques offered valuable experimental evidences of, for example, the superconducting electron pairing state and the effect of electron-electron correlations. These techniques are still widely used on the new discovered superconductor families like alkali doped fullerens, iron-pnictides, with an aim of providing enough experimental data to help the development of the complete theory of superconductivity.

References

[1] Superconductivity, Wikipedia, available on-line: http://en.wikipedia.org/wiki/Superconductivity (cited on 27. 02. 2010).

[2] M. Weger. "NMR in Superconductors". Pure Appl. Chem. **32**, 325 (1977).

[3] J. G. Bednorz and K. A. Mueller, Z. Phys. **B64**, 189 (1986).

[4] W. Heitler and E. Teller, Proc. Roy. Soc. A **155,** 629 (1936).

[5] J. Korringa, Physica **16**, 601 (1950).

[6] D. F. Smith and C. P. Slichter, "The Study of Mechanisms of Superconductivity by NMR Relaxation", Lect. Notes Phys. **684**, 243 (2006).

[7] Takabayashi, et.al., Science **323**, 1585 (2009).

[8] W. D. Knight, Phys. Rev. **76**, 1259 (1949).

[9] C. P. Slichter. "Principles of Magnetic Resonance". (Springer-Verlag Berlin Heidelberg New York 1990).

[10] R. E. Norberg, C. P. Slichter, Phys. Rev. **83**, 1074 (1951).

[11] D. Pines, Solid State Physics, Vol. 1 Chapter Electron interaction in metals. (Academic, New York 1955) p. 367.

[12] J. F. Annett, Superconductivity, Superfluids and Condensates (Oxford Universitly Press 2004)

[13] V. L. Ginzburg and L. D. Landau, Zh. Experim. I Theor. Piz. **20**, 1064 (1959).

[14] A. B. Pippard, Proc. Roy. Soc. A **216**, 547 (1935).

[15] A. A. Abrikosov, Zh. Eksperim. i Teor. Fiz. **32**, 1442 (1957).

[16] A. G. Redfield, Phys. Rev. **162**, 367 (1967).

[17] H. F. Hess, et. al., Phys. Rev. Lett. **65**, 214 (1989).

[18] W. fite and A. G. Redfield, Phys. Rev. Lett. **17**, 381 (1966).

[19] B. G. Silbernagel, et.al., Phys. Rev. Lett. **17**, 384 (1966).

[20] L. C. Hebel and C. P. Slichter, Phys. Rev. **113**, 1504 (1959).

[21] M. A. Wolf and F. Reif, Phys. Rev. **137A**, 557 (1965).

[22] V. Hoffstein and R. Cohen, Phys. Lett. **29A**, 603 (1969). M. Weger, Solid State Comm. **9**, 107 (1971).

[23] J. Bardeen and D. Pines, Phys. Rev. **99**, 1140 (1955).

[24] D. A. Wolman et.al., Phys. Rev. Lett. **71**, 2134 (1993).

[25] A. F. Hebard, et al., Nature **350**, 600 (1991).

[26] C. H. Pennington and V. A. Stenger, Rev. Mod. Phys. **66**, 855 (1996).

[27] R. Tycko et.al., Phys. Rev. Lett. **68**, 1912 (1992).

[28] V. A. Stenger et.al., Phys. Rev. Lett. **74**, 1649 (1995).

[29] P. Jeglič et. al., Phys. Rev. B 80, 195424 (2009).

[30] Y. Masuda and N. Okuba, Phys. Rev. Lett **20**, 1475 (1968).

[31] N. J. Curro et.al., Phys. Rev. B **56**, 877 (1997).

[32] T. Imai, et.al., Phys. Soc. Jpn. **63**, 700 (1994).

[33] J. A. Martindale et.al., Phys. Rev. B **47**, 9155 (1993).